Journal of Sound and Vibration (1997) **208**(4), 501–516

THE FREE VIBRATION OF LONG-SPAN TRANSMISSION LINE CONDUCTORS WITH DAMPERS

H. Q. Wang, J. C. Miao, J. H. Luo, F. Huang and L. G. Wang

Department of Engineering Mechanics, Huazhong University of Science and Technology, Wuhan, Hubei, People's Republic of China

(*Received* 12 *June* 1996, *and in final form* 18 *June* 1997)

The free vibration of a transmission line conductor equipped with a number of Stockbridge dampers is modelled by a differential equation of motion of a tensioned beam acted on by concentrated frequency dependent forces, and an exact solution is obtained using integral transformation. By evaluation through aeolian vibration level computation, the expressions obtained for the mode shapes can be easily used to predict accurately the overall strains of lines in operation or under design. Numerical examples show that the usual sinusoidal mode shapes can be significantly distorted by the dampers to give rise to dangerous strains.

1. INTRODUCTION

Aeolian vibration of electrical transmission line conductors due to oscillatory lift force actions caused by vortex shedding gives rise to material fatigue in a wide wind speed range (1–10 m/s). The subject has invited a great number of investigations. Excellent reviews are found in the Shock and Vibration Digest [1] and elsewhere [2].

Suitable damping devices like symmetric and asymmetric Stockbridge dampers are successfully used to bring down the induced strains of the conductors near the suspension clamps. For a long-span conductor, quite a few dampers, for instance, six at each end, are needed. Since the spacing of the neighbouring frequencies is of the order of 0·08 Hz or less for a span over 1000 m long, the aeolian vibration spectrum can be regarded as almost continuous. The stagger protective frequency ranges of different types of dampers may serve to cover entirely the almost continuous spectrum. Under the protection of so many well-developed dampers, the conductor in the vicinity of the suspension clamps may work with safety, while cases are known in which damage is observed at the points of attachment of the dampers, specially the one farthest from the suspension clamp it protects. Analysis concerning what actually happens to these points is rarely found in literature. In investigations that have reported studies of the response of a cable with dampers, concepts such as sine-shaped loops, i.e., the mode shapes of a string or a beam, are often used to represent the mode shapes of the cable, without taking into consideration distortion due to the dampers. Some studies have neglected the bending stiffness of the cable and thus no conclusion of stress and strain can be formed. As reasonably suggested in reference [3], sufficient attention should be given to good modelling of this aspect of the problem. On the other hand, methods of estimating the aeolian response are available today, and it is possible to design transmission lines with more operational safety with the

0022–460X/97/490501 + 16 $25.00/0/sv971196

help of these methods. They can be grouped under two headings. Firstly, the aeolian vibration levels of the span are determined from the energy balance [3–5] by using quantitative relationships between vibration level and wind power input, conductor self damping power dissipation, and external damper power dissipation. Secondly, the behaviour of the wind-excited lift is assumed to satisfy empirical models based on experimental data. The modelling effort was initiated by Hartlen and Currie [6] and improved and extended to be applicable to elastic cylinders like transmission line conductors by Iwan [7] and Skop and Griffin [8] separately and reviewed by Tsui [2]. In either of the two groups, mode shapes of the cable are required. If the computation is intended for part of a practical industrial design, the most important results should be the dynamic stresses or strains of the cable at the dangerous points, i.e., points of attachment of the dampers and the suspension clamps. Mode shapes that come out of approximate methods such as the Ritz–Galerkin method or discrete methods such as FEM are not likely to be adequate for these purposes, since the aeolian frequency range of 8–80 Hz of a long span (over 1000 m in length and around 30 mm in diameter) corresponds to orders as high as 100–1000th and it is well known that the computational error of approximate methods increases rapidly with a rise in order. The most reliable procedure may be conducted by applying the four continuity conditions for each two consecutive sections adjacent to one damper so as to formulate a transfer matrix. However, such a procedure is quite time consuming if multiple dampers are involved in view of the fact that choice of characteristic (tuning) and location of dampers is an inverse problem of vibration. In this investigation a long-span transmission line conductor equipped with multiple dampers is modelled as a highly tensioned straight beam acted on by concentrated frequency dependent forces. Exact and explicit expressions for frequency equations and mode shapes are obtained via integral transformation. It is worth mentioning and extremely interesting that by a special arrangement in the solution, most terms in the expressions are eliminated so that the remains are computable and quite time saving.

2. GOVERNING EQUATION AND SOLUTION

As determined in reference [9], for frequencies in the aeolian spectrum, the description of the transverse dynamics of taut catenary conductors is given accurately enough by the straight tensioned beam partial differential equation, which is well known as

$$EJ\frac{\partial^4 y}{\partial x^4} - S\frac{\partial^2 y}{\partial x^2} + M\frac{\partial^2 y}{\partial t^2} = \sum_{i=1}^{n} p_i\,\delta(x - x_i). \tag{1}$$

In equation (1) $y(x, t)$ is the transverse dynamic displacement of the point at a distance x to one of the two extremities of the span and at time t, EJ is the bending stiffness of the cable determined experimentally, S is the tension, M is the mass per unit length, and p_i as a function of frequency is the force exerted by the ith damper on the conductor. It is understood that moments introduced by a damper are of no importance to the overall vibration behaviour and are thus neglected. n is the number of the dampers used in the vicinity of this extremity of the span. Since dampers are used equal in number and equally spaced from the two extremities, the property of symmetry of the span exists and is of great importance to the computation for the computational volume increases drastically with a rise in number of dampers. δ is the first type of spatial Dirac's delta function and x_i are the locations of the dampers as shown in Figure 1. The moments of the dampers can be taken into consideration in terms of the second type of Dirac's delta function but the

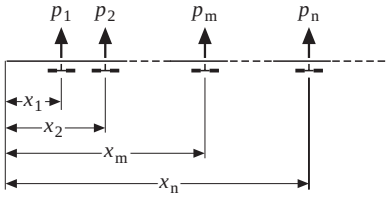

Figure 1. Locations of the dampers.

computation would be much more lengthy. Equation (1) is valid for $x \leqslant L$, where L is the length of half span. The boundary conditions at $x = 0$ are

$$y(0, t) = 0, \qquad y''(0, t) = 0, \tag{2}$$

for hinged ends, as described in Section 4, and

$$y(0, t) = 0, \qquad y'(0, t) = 0, \tag{3}$$

for clamped ends, where primes stand for differentiation with respect to x. At $x = L$ one has

$$y(L, t) = 0, \qquad y''(L, t) = 0, \tag{4}$$

for even orders or antisymmetric mode shapes and

$$y'(L, t) = 0, \qquad y'''(L, t) = 0, \tag{5}$$

for odd orders or symmetric mode shapes.

By assuming a solution to equation (1) in the form

$$y(x, t) = Y(x)\eta(t), \tag{6}$$

in which the generalized co-ordinate $\eta(t)$ is determined by

$$\mathrm{d}^2\eta/\mathrm{d}t^2 + \omega^2\eta = 0, \tag{7}$$

of which the solution is sinusoidal, the mode shape $Y(x)$ is determined by

$$\frac{\mathrm{d}^4 Y}{\mathrm{d}x^4} - \frac{S}{EJ}\frac{\mathrm{d}^2 Y}{\mathrm{d}x^2} - \frac{\omega^2 M}{EJ}\,Y = \frac{1}{EJ}\sum_{i=1}^{n} P_i\,\delta(x - x_i), \tag{8}$$

with ω the corresponding natural circular frequency to be determined. In (8) P_i is the amplitude of the sinusoidal force p_i.

It is convenient to handle both sides of equation (8) with the Karson transform [10]

$$K[Y(x)] = X(\sigma) = \sigma \int_0^\infty \mathrm{e}^{-\sigma x} Y(x)\,\mathrm{d}x, \tag{9}$$

where $K[Y]$ is the Karson transform of the spatial function Y, and σ is the Karson operator. The relationship (9) can be denoted as

$$X(\sigma) \rightarrow Y(x) \tag{10}$$

and immediately yields

$$\sigma^k[X(\sigma) - Y(0) - (1/\sigma)Y'(0) - \cdots - (1/\sigma^{k-1})Y^{(k-1)}(0)] \rightarrow Y^{(k)}(x). \tag{11}$$

By denoting $F(\sigma) \rightarrow f(x) = EJ\Sigma_{i=1}^{m} P_i\,\delta(x - x_i)$, in which $m = 1, 2, \ldots, n$, the solution to equation (8) in the Karson domain is

$$X(\sigma) = [1/(\sigma^4 - (S/EJ)\sigma^2 - \omega^2 M/EJ)][Y(0)(\sigma^4 - (S/EJ)\sigma^2) + Y'(0)(\sigma^3 - (S/EJ)\sigma) + Y''(0)\sigma^2 + Y'''(0)\sigma + F(\sigma)]. \tag{12}$$

The fraction in front of the bracket can be handled by assuming

$$S/EJ = \beta^2 - \alpha^2, \qquad \omega^2 M/EJ = \beta^2\alpha^2$$

and an inverse Karson transform turns the last term to

$$\frac{1}{\sigma^2 - (S/EJ)\sigma^2 - \omega^2 M/EJ} F(\sigma) = \frac{1}{\beta^2 + \alpha^2}\left(\frac{1}{\sigma}\frac{1}{\beta}\frac{F(\sigma)\sigma\beta}{\sigma^2 - \beta^2} - \frac{1}{\sigma}\frac{1}{\alpha}\frac{F(\sigma)\sigma\alpha}{\sigma^2 + \alpha^2}\right)$$

$$\rightarrow \frac{1}{\beta^2 + \alpha^2}\left[\frac{1}{\beta}\int_0^x f(\xi)\,\mathrm{sh}\,\beta(x - \xi)\,\mathrm{d}\xi - \frac{1}{\alpha}\int_0^x f(\xi)\sin\alpha(x - \xi)\,\mathrm{d}\xi\right]$$

$$= \frac{1}{\beta^2 + \alpha^2}\frac{1}{EJ}\sum_{i=1}^{m} P_i\left[\frac{1}{\beta}\,\mathrm{sh}\,\beta(x - x_i) - \frac{1}{\alpha}\sin\alpha(x - x_i)\right],$$

$$x_m \leqslant x \leqslant x_{m+1},\ m = 1, 2, \ldots, n. \tag{13}$$

which vanishes where $x < x_1$. One applies the same procedure to each term of equation (12) and obtain the solution for equation (8):

$$Y(x) = Y(0)S(x) + Y'(0)T(x) + Y''(0)U(x) + Y'''(0)V(x) + G\sum_{i=1}^{m} P_i\,V(x - x_i),$$

$$x_m \leqslant x \leqslant x_{m+1}, \qquad m = 1, 2, \ldots, n. \tag{14}$$

excluding a common factor $1/(\beta^2 + \alpha^2)$, with the last term vanishing where $x < x_1$. In equation (14),

$$S(x) = \alpha^2\,\mathrm{ch}\,\beta x + \beta^2\cos\alpha x, \qquad T(x) = (\alpha^2/\beta)\,\mathrm{sh}\,\beta x + (\beta^2/\alpha)\sin\alpha x,$$

$$U(x) = \mathrm{ch}\,\beta x - \cos\alpha x, \qquad V(x) = (1/\beta)\,\mathrm{sh}\,\beta x - (1/\alpha)\sin\alpha x, \tag{15}$$

may be referred to as generalized Krylov functions for tensioned beams, and $G = 1/EJ$. According to the above definition of α and β,

$$\alpha = \sqrt{-S/2EJ + \tfrac{1}{2}\sqrt{(S/EJ)^2 + 4\,\omega^2 M/EJ}},$$

$$\beta = \sqrt{S/2EJ + \tfrac{1}{2}\sqrt{(S/EJ)^2 + 4\,\omega^2 M/EJ}}. \tag{16}$$

A Stockbridge damper is supposed to have a linear characteristic so that a harmonic linear motion of the damper clamp generates a harmonic force on the conductor it protects, and the amplitude P_i of the force is proportional to that of the displacement of its clamp, i.e.,

$$P_i = Y(x_i)q_i, \tag{17}$$

in which q_i as a frequency function is a characteristic of the ith damper and referred to as force response by Claren and Diana [12]. For an asymmetric damper the force response can be determined experimentally or modelled as a four-degree-of-freedom spring–mass system as shown in [11] and described briefly in the Appendix. As usual, damping in the dampers as well as in the conductor cable is neglected in this free vibration analysis since it gives no significant effects on natural frequencies and mode shapes. A so-called damper thus works as four dynamic absorbers without damping.

Now the local amplitudes $Y(x_i)$ are involved in expression (14). Each of them can be expressed using the expression itself in terms of the local amplitudes of the dampers closer to the origin $x = 0$:

$$Y(x_i) = Y(0)S(x_i) + Y'(0)T(x_i) + Y''(0)U(x_i) + Y'''(0)V(x_i)$$

$$+ G\sum_{j=1}^{i-1} q_j\, Y(x_j)V(x_i - x_j). \tag{18}$$

This expression is used successively to give

$$Y(x) = Y'(0)\left[T(x) + G^m \sum_{s=1}^{m} \sum\nolimits_j Q_j\, V_j\, T(x_{js})V(x - x_{j1})\right]$$

$$+ Y'''(0)\left[V(x) + G^m \sum_{s=1}^{m} \sum\nolimits_j Q_j\, V_j\, V(x_{js})V(x - x_{j1})\right]$$

$$x_m \leqslant x \leqslant x_{m+1}, \qquad m = 1, 2, \ldots, n, \tag{19}$$

for boundary conditions (2) and

$$Y(x) = Y''(0)\left[U(x) + G^m \sum_{s=1}^{m} \sum\nolimits_j Q_j\, V_j\, U(x_{js})V(x - x_{j1})\right]$$

$$+ Y'''(0)\left[V(x) + G^m \sum_{s=1}^{m} \sum\nolimits_j Q_j\, V_j\, V(x_{js})V(x - x_{j1})\right],$$

$$x_m \leqslant x \leqslant x_{m+1}, \qquad m = 1, 2, \ldots, n, \tag{20}$$

for (3), where

$$\sum\nolimits_j = \sum_{\substack{j1=1 \\ j1 > j2 > \cdots js}}^{m} \sum_{j2=1}^{m} \cdots \sum_{js=1}^{m}, \qquad Q_j = q_{j1}\, q_{j2} \ldots q_{js},$$

$$V_j = V(x_{j1} - x_{j2})V(x_{j2} - x_{j3}) \ldots V(x_{j(s-1)} - x_{js}), \tag{21}$$

with $V_j = 1$ for $s = 1$. Here single subscripts are replaced by double subscripts so that the latter can be distinguished from what follows, i.e., $q_1, q_2, \ldots, q_n$, and $x_1, x_2, \ldots, x_n$ are replaced by $q_{j1}, q_{j2}, \ldots, q_{jm}$ and $x_{j1}, x_{j2}, \ldots, x_{jm}$, $m = 1, 2, \ldots, n$, respectively.

In expressions (19) and (20) it is obvious that a great number of terms contain factors in the form of $\exp(\beta \sum_k x_k)$. For usual long spans β is above 7 so that the value of an exponential function like this may become extremely large once the exponent, or the summation, appears to be positive. It can be shown also that this is the case with more than half of the terms. What is worse is that the evaluation of these functions by computers gives rise to significant errors so that the results would be absolutely preposterous. Expressions involving functions with positive exponents must be regarded as incomputable. In what follows, terms with positive exponents are called super terms. It is essential to show how super terms can be eliminated under a certain arrangement.

3. BOUNDARY CONDITIONS AND ELIMINATION OF SUPER TERMS, NATURAL FREQUENCIES AND MODE SHAPES

As usual, boundary conditions are used to determine the integral constants in equations (19) and (20). To eliminate the super terms at the same time, one arranges to use the boundary conditions in a special way. Boundary conditions for hinged ends (2) and (4) will be taken for an example. Boundary conditions other than (2) and (4) result in much more lengthy expressions for mode shapes and frequency equations. This contrast is similar to that in the case of usual beam-alone and tension-free models where expressions for hinged beams are much simpler than those for other kinds of beams.

One now uses (2) and (4) as:

$$Y(L)\beta^2 - Y''(L) = 0:$$

$$Y'(0)\left[\beta^2 \sin \alpha L - \sum_{r=1}^{n} G^r \sum_i Q_i V_i T(x_{ir}) \sin \alpha(L - x_{i1})\right]$$

$$+ Y'''(0)\left[-\sin \alpha L - \sum_{r=1}^{n} G^r \sum_i Q_i V_i V(x_{ir}) \sin \alpha(L - x_{i1})\right] = 0; \tag{22}$$

$$Y(L)\alpha^2 + Y''(L) = 0:$$

$$Y'(0)\left[\alpha^2(e^{\beta L} - e^{-\beta L}) + \sum_{r=1}^{n} G^r \sum_i Q_i V_i T(x_{ir}) (e^{\beta(L - x_{i1})} - e^{-\beta(L - x_{i1})})\right],$$

$$+ Y'''(0)\left[e^{\beta L} - e^{-\beta L} + \sum_{r=1}^{n} G^r \sum_i Q V_i V(x_{ir}) e^{\beta(L - x_{i1})} - e^{-\beta(L - x_{i1})})\right] = 0, \tag{23}$$

in which running subscripts j and s in (21) are replaced by i and r respectively running through the whole half span with $m = n$ and $x = L$, and some of the hyperbolic functions are replaced by exponential functions for the sake of convenient elimination of the super terms.

One of the two equations may serve to relate the two constants $Y'(0)$ and $Y'''(0)$ and the other would serve as the frequency equation. Hence one has

$$Y'''(0) = -Y'(0)\left(\alpha^2 + \sum_{r=1}^{n} G^r \sum_i Q_i \bar{V}_i T(x_{ir})\, e^{-\beta x_{ir}}\right)\Big/\left(1 + \sum_{r=1}^{n} G^r \sum_i Q_i \bar{V}_i T(x_{ir})\, e^{-\beta x_{ir}}\right), \tag{24}$$

in which the extremely small quantities $e^{-2\beta L}$ and $e^{-\beta(2L - x_{i1})}$ are omitted. In (24) the following notations have been introduced:

$$\begin{aligned}\bar{V}_i &= V_i / e^{\beta(x_{i1} - x_{ir})} = \bar{V}(x_{i1} - x_{i2})\bar{V}(x_{i2} - x_{i3}) \ldots \bar{V}(x_{i(r-1)} - x_{ir}) \\ &= [1/2\beta - (1/2\beta)\, e^{-2\beta(x_{i1} - x_{i2})} - (1/\alpha)\, e^{-\beta(x_{i1} - x_{i2})} \sin \alpha(x_{i1} - x_{i2})] \\ &\quad \times [1/2\beta - (1/2\beta)\, e^{-2\beta(x_{i2} - x_{i3})} - (1/\alpha)\, e^{-\beta(x_{i2} - x_{i3})} \sin \alpha(x_{i2} - x_{i3})] \\ &\quad \times \ldots \times [1/2\beta - (1/2\beta)\, e^{-2\beta(x_{i(r-1)} - x_{ir})} - (1/\alpha)\, e^{-\beta(x_{i(r-1)} - x_{ir})} \sin \alpha(x_{i(r-1)} - r_{ir})].\end{aligned} \tag{25}$$

A similar expression for $\bar{V}_j$ can be written by replacing i with j and r with s. Hereafter super terms will appear elsewhere, i.e., not in $\bar{V}_i$, $\bar{V}_j$.

Now from equation (22) one obtains

$$\begin{aligned}&\left[1 + \frac{1}{2\beta}\sum_{r=1}^{n} G^r \sum_i Q_i \bar{V}_i (1 - e^{-2\beta x_{ir}})\right] \sin \alpha L \\ &\quad - \frac{1}{\alpha}\sum_{r=1}^{n} G^r \sum_i Q_i \bar{V}_i\, e^{\beta(x_{i1} - x_{ir})} \sin \alpha x_{ir} \sin \alpha(L - x_{i1}) \\ &\quad - \frac{1}{2\beta\alpha}\sum_{r=1}^{n}\sum_{s=1}^{n} G^r G^s \sum_i \sum_j Q_i Q_j \bar{V}_i \bar{V}_j [e^{\beta(x_{j1} - x_{js})(1 - e^{-2\beta x_{ir}})} \sin a x_{js} \\ &\quad - e^{\beta(x_{j1} - x_{ir})}(1 - e^{-2\beta x_{js}}) \sin \alpha(L - x_{j1})] = 0\end{aligned} \tag{26}$$

as the frequency equation. A value of ω is a natural circular frequency of the span if it yields a pair of α and β according to equation (16) that make the left side of equation (26) vanish.

In (26) one sees that possible super terms may take place where the explicit exponentials are positive, and no super terms may possibly appear elsewhere, e.g., in the first term of the three terms of the equation. One will show later how the super terms are eliminated.

For long spans frequency equations are far less important than expressions of mode shapes since the frequency spectra are almost continuous. As for the mode shapes, one obtains from equations (19) and (24)

$$\begin{aligned}Y(x) = A(m) \sin \alpha x + B(m) \cos \alpha x + C(m)\, e^{\beta(x - x_{m+1})} + D(m)\, e^{-\beta(x - x_m)}, \\ x_m \leqslant x \leqslant x_{m+1},\ m \leqslant n,\end{aligned} \tag{27}$$

where

$$A(m) = 1 + \frac{1}{2\beta}\sum_{r=1}^{n} G^r \sum_i Q_i \bar{V}_i (1 - e^{-2\beta x_{ir}}) - \frac{1}{\alpha}\sum_{s=1}^{m} G^s \sum_j Q_j \bar{V}_j\, e^{(x_{j1} - x_{js})} \sin \alpha x_{js} \cos \alpha x_{j1}$$

$$- \frac{1}{2\beta\alpha} \sum_{r=1}^{n} \sum_{s=1}^{m} G^r G^s \sum_i \sum_j Q_i Q_j \bar{V}_i \bar{V}_j \Big[e^{\beta(x_{j1} - x_{js})}(1 - e^{-2\beta x_{ir}}) \sin \alpha x_{js}$$

$$- e^{\beta(x_{j1} - x_{js})}(1 - e^{-2\beta x_{js}}) \sin \alpha x_{ir} \Big] \cos \alpha x_{j1}, \tag{28}$$

$$B(m) = \frac{1}{\alpha} \sum_{s=1}^{m} G^s \sum_j Q_j \bar{V}_j e^{\beta(x_{j1} - x_{js})} \sin \alpha x_{js} \sin \alpha x_{j1}$$

$$+ \frac{1}{2\beta\alpha} \sum_{r=1}^{n} \sum_{s=1}^{m} G^r G^s \sum_i \sum_j Q_i Q_j \bar{V}_i \bar{V}_j \Big[e^{\beta(x_{j1} - x_{js})}(1 - e^{-2\beta x_{ir}}) \sin \alpha x_{js}$$

$$- e^{\beta(x_{j1} - x_{ir})}(1 - e^{-2\beta x_{js}}) \sin \alpha x_{ir} \Big] \sin \alpha x_{j1}, \tag{29}$$

$$C(m) = -\frac{1}{2\beta} \sum_{r=1}^{n} G^r \sum_i Q_i \bar{V}_i \ e^{\beta(x_{m+1} - x_{ir})} \sin \alpha x_{ir}$$

$$+ \frac{1}{2\beta} \sum_{s=1}^{m} G^s \sum_j Q_j \bar{V}_j e^{\beta(x_{m+1} - x_{js})} \sin \alpha x_{js}$$

$$+ \frac{1}{(2\beta)^2} \sum_{r=1}^{n} \sum_{s=1}^{m} G^r G^s \sum_i \sum_j Q_i Q_j \bar{V}_i \bar{V}_j \left[e^{\beta(x_{m+1} - x_{js})}(1 - e^{-2\beta x_{ir}}) \sin \alpha x_{js} \right.$$

$$\left. - e^{\beta(x_{m+1} - x_{ir})}(1 - e^{-2\beta x_{js}}) \sin \alpha x_{ir} \right], \tag{30}$$

$$D(m) = \frac{1}{2\beta} \sum_{r=1}^{n} G^r \sum_i Q_i \bar{V}_i e^{-\beta(x_m + x_{ir})} \sin \alpha x_{ir}$$

$$- \frac{1}{2\beta} \sum_{s=1}^{m} G^s \sum_j Q_j \bar{V}_j e^{\beta(-x_m + 2x_{j1} - x_{js})} \sin \alpha x_{js} \tag{31}$$

$$- \frac{1}{(2\beta)^2} \sum_{r=1}^{n} \sum_{s=1}^{m} G^r G^s \sum_i \sum_j Q_i Q_j \bar{V}_i \bar{V}_j \Big[e^{\beta(-x_m + 2x_{j1} - x_{js})}(1 - e^{-2\beta x_{ir}}) \sin \alpha x_{js}$$

$$- e^{\beta(-x_m + 2x_{j1} - x_{ir})}(1 - e^{-2\beta x_{js}}) \sin \alpha x_{ir} \Big], \tag{31}$$

with $x_{n+1} = L$.

In the coefficients A, B, C and D and also in equation (26), possible super terms take place where the explicit exponentials are positive, including expressions like $e^{\beta(x_{j1} - x_{js} - 2x_{ir})}$. One starts with $A(m)$ to show how they are eliminated. Table 1 displays the running subscripts in the case $n = 3$ and $m = 2$ as an example.

TABLE 1

Elimination of explicit super terms that appear in equation (28) *for* $n = 3$, $m = 2$

r	i series		s = 1, $j1 = js$		s = 2, $j1 \quad j2 = js$			
			1	2	+	2	1	<3>
1	$i1 = ir$	1	1,1 <1>	+ 1,2 <3>	+	1,21		<1>
		2	2,1	2,2 <1>	+	2,21		<2>
		3	3,1	3,2	+	3,21		<3>
2	$i1$ $i2 = ir$	2 1	21,1 <1>	+ 21,2 <2>	+	21,21		<1>
	$i1$ $i2 = ir$	3 1	31,1 <1>	+ 31,2 <3>	+	31,21		<1>
	$i1$ $i2 = ir$	3 2	32,1	32,2 <1>	+	32,21		<2>
3	$i1$ $i2$ $i3 = ir$	3 2 1	321,1 <1>	+ 321,2 <2>	+	321,21		<1>

In Table 1, the figures between the two vertical double lines are subscripts that appear in the second term of the four terms of (28), those between the two horizontal double lines are what appear in the third term, and those in the 7×3 matrix are what appear in the fourth term.

Super terms appear in squares marked with $+$, with commas separating the i series and j series. For example 1,21 implies $ir = i1 = 1$; $j1 = 2$, $js = j2 = 1$. In the explicit exponentials in the corresponding bracket in (28), there are 4 possible super terms, namely, in sequence,

$$e^{\beta(x_2 - x_1)},\ e^{\beta(x_2 - x_1 - 2x_1)},\ e^{\beta(x_2 - x_1)} \quad \text{and} \quad e^{\beta(x_2 - x_1 - 2x_1)}.$$

Multiplied by terms in $\bar{V}_i$ and $\bar{V}_j$, which are now $\bar{V}_i = 1$ for $r = 1$ and

$$\bar{V}_j = \frac{V(x_{j1} - x_{j2})}{e^{\beta(x_{j1} - x_{j2})}} = \frac{1}{2\beta} - \frac{1}{2\beta} e^{-2\beta(x_2 - x_1)} - \frac{1}{\alpha} e^{-\beta(x_2 - x_1)} \sin \alpha(x_2 - x_1)$$

for $s = 2$, yielding four possible final super terms, namely, their products with $1/2\beta$. Possible super terms are regarded as super terms to be eliminated.

The super terms are eliminated in two different ways. In squares where at least two figures are duplicate, super terms always appear in couples. The partners in each couple have the same magnitudes and opposite signs so as to be eliminated. They are marked with $\langle 2 \rangle$ in Table 1. For example, 32,21 ($r = 2$, $s = 2$) implies a term

$$-(1/2\beta\alpha)G^2G^2q_3\, q_2\, q_2\, q_1\, \bar{V}(x_3 - x_2)\bar{V}(x_2 - x_1)$$
$$\times [e^{\beta(x_2 - x_1)}(1 - e^{-2\beta x_2}) \sin \alpha x_1 - e^{\beta(x_2 - x_2)}(1 - e^{-2\beta x_1}) \sin \alpha x_2]$$

Its counterpart is found to be 321,2 ($r = 3$, $s = 1$):

$$-(1/2\beta\alpha)\, G^3 G q_3\, q_2\, q_1\, q_2\, \bar{V}(x_3 - x_2)\bar{V}(x_2 - x_1)$$
$$\times [e^{\beta(x_2 - x_2)}(1 - e^{-2\beta x_1}) \sin \alpha x_2 - e^{\beta(x_2 - x_1)}(1 - e^{-2\beta x_2}) \sin \alpha x_1].$$

Actually these two terms yield each other by exchanging the duplicate figures (2 and 2) and figures following them (21 and 12), with the products of $\bar{V}_i\, \bar{V}_j$ remaining unchanged. During the exchange the figure $j1$ remains the same and the symmetry between ir and js in the bracket guarantees the elimination. An exceptional but even simpler elimination takes place when in one term $ir = js$, and the term itself vanishes, for example 321,1.

In the cases where no duplicate subscripts occur, the elimination of super terms is more complicated. The only examples for $n = 3$, $m = 2$ are 3,21;31,2; and 21;1,2. In 32,1 duplication does not occur, but no super term occurs either. 321 in the i series appears in the second term of (28) so it does not give rise to super terms. When no duplicate subscripts occur, all the super terms for the specific m must be put together for elimination. For 3,21;31,2, one has

$$-\frac{1}{2\beta\alpha}\, G G^2 q_3\, q_2\, q_1 \left[\frac{1}{2\beta} - \frac{1}{2\beta}\, e^{-2\beta(x_2 - x_1)} - \frac{1}{\alpha}\, e^{-\beta(x_2 - x_1)} \sin \alpha(x_2 - x_1)\right]$$
$$\times [e^{\beta(x_2 - x_1)}(1 - e^{-2\beta x_3}) \sin \alpha x_1 - e^{\beta(x_2 - x_1)}(1 - e^{-2\beta x_1}) \sin \alpha x_3] \cos \alpha x_2,$$

and

$$-\frac{1}{2\beta\alpha}\, G^2 G q_3\, q_1\, q_2 \left[\frac{1}{2\beta} - \frac{1}{2\beta}\, e^{-2\beta(x_3 - x_1)} - \frac{1}{\alpha}\, e^{-\beta(x_3 - x_1)} \sin \alpha(x_3 - x_1)\right]$$
$$\times [e^{\beta(x_2 - x_2)}(1 - e^{-2\beta x_1}) \sin \alpha x_2 - e^{\beta(x_2 - x_1)}(1 - e^{-2\beta x_2}) \sin \alpha x_1] \cos \alpha x_2,$$

the final super terms being

$$-(1/2\beta\alpha) G^3 q_3\, q_2\, q_1\, [(1/2\beta)\, e^{\beta(x_2 - x_1)} \sin \alpha x_1] \cos \alpha x_2$$

and

$$-(1/2\beta\alpha) G^3 q_3\, q_1\, q_2\, [-(1/2\beta)\, e^{\beta(x_2 - x_1)} \sin \alpha x_1] \cos \alpha x_2,$$

respectively, and hence the elimination. For 21;1,2 with the former in the third term and the latter in the fourth term of equation (28), one has

$$-\frac{1}{\alpha}\, G^2 q_2\, q_1 \left[\frac{1}{2\beta} - \frac{1}{2\beta}\, e^{-2\beta(x_2 - x_1)} - \frac{1}{\alpha}\, e^{-\beta(x_2 - x_1)} \sin \alpha(x_2 - x_1)\right] e^{\beta(x_2 - x_1)} \sin \alpha x_1 \cos \alpha x_2$$

and

$$-\frac{1}{2\beta\alpha}\, G G q_1\, q_2 \left[e^{2\beta(x_2 - x_2)}(1 - e^{-2\beta x_1}) \sin \alpha x_2 - e^{\beta(x_2 - x_1)}(1 - e^{-2\beta x_2}) \sin \alpha x_1\right] \cos \alpha x_2.$$

The final super terms being

$$-(1/\alpha) G^2 q_2\, q_1\, [(1/2\beta)\, e^{\beta(x_2 - x_1)} \sin \alpha x_1 \cos \alpha x_2]$$

TABLE 2

Elimination of explicit super terms that appear in equation (30) *for* $n = 3$, $m = 2$

r	i series	s / j series	1			2				
			$j1 = js$			$j1$	$j2 = js$			
			+ 1	<4>		+ 2	<4>	+ 2	1	<4>
1	$i1 = ir$	+ 1 <4>	+ 1,1	<1>		+ 1,2	<4>	+	1,21	<1>
		+ 2 <4>	+ 2,1	<4>		+ 2,2	<1>	+	2,21	<2>
		3	+ 3,1	<3>		+ 3,2	<3>	+	3,21	<3>
2	$i1$ $i2 = ir$	+ 2 <4> 1	+ 21,1	<1>		+ 21,2	<2>	+	21,21	<1>
	$i1$ $i2 = ir$	+ 3 <3> 1	+ 31,1	<1>		+ 31,2	<3>	+	31,21	<1>
	$i1$ $i2 = ir$	+ 3 <3> 2	+ 32,1	<3>		+ 32,2	<1>	+	32,21	<2>
3	$i1$ $i2$ $i3 = ir$	+ 3 <3> 2 1	+ 321,1	<1>		+ 321,2	<2>	+	321,21	<1>

and

$$-(1/\alpha)G^2 q_1 q_2 \left[-\frac{1}{2\beta} e^{\beta(x_2 - x_1)} \sin \alpha x_1 \right] \cos \alpha x_2,$$

respectively, and hence the elimination. For $m > 2$, more than two terms are put together for elimination.

In practical computation, no attention need be payed to the elimination. In computing each term in expressions (28)–(31), one simply asks the computer to judge sequentially $\langle 1 \rangle$ whether $ir = js$ (easier for computer than the next two steps), $\langle 2 \rangle$ whether duplicate figures occur (easier than the next step) and $\langle 3 \rangle$ whether the final exponential is positive. Each positive answer to these three questions results in cancellation of the term under consideration. Three negative answers causes execution of the computation of the term.

Identical constructions exist in expressions (28), (29) and (31) for $A(m)$, $B(m)$ and $D(m)$ and the frequency equation (26), so the elimination of super terms in $B(m)$, $D(m)$ and the

TABLE 3

Natural frequencies of the four types of dampers

Type	Natural frequency (Hz)			
I	12·49	38·80	20·50	70·03
II	14·50	60·00	30·00	90·00
III	16·99	66·00	35·01	95·96
IV	16·99	74·00	35·01	99·95

TABLE 4

Parameters of the four types of dampers

Type	Parameters									
	I_1 (kg/m)	I_2	M_1 (kg)	M_2	K_1 (N/m)	K_2	L_1 (m)	L_2	e_1 (m)	e_2
I	0·0118	0·00314	3·33	2·65	16425	30102	0·20	0·15	0·03	0·025
II	0·00286	0·00272	1·94	1·45	11076	38651	0·20	0·15	0·03	0·025
III	0·00179	0·00256	1·03	0·842	8233·2	35556	0·20	0·15	0·03	0·025
IV	0·00117	0·0017	0·904	0·723	6997·9	27893	0·20	0·15	0·03	0·025

Notation defined in the Appendix.

TABLE 5

Arrangement of dampers

Location x_i (m)	Type		
	Figs. 2, 3, 4	Figs. 5, 6, 7	Fig. 8
0·8	I	I	I
2·4	II	II	II
4·0	III	III	III
5·8	IV	II	II
7·6	–	III	III
9·6	–	–	IV

frequency equation can be done in the same way. As for the super terms in $C(m)$, they are eliminated in a slightly different way as follows.

Table 2 has been constructed for the subscripts that appear in $C(m)$, also for $n = 3$, $m = 2$. One sees that 30 terms instead of 12 (in Table 1) out of 31 are explicit super terms marked with $+$, owing to the fact that $x_{m+1} > x_{j1}$. However, one more facility is available for elimination, namely, the entire symmetry between x_{ir} and x_{js} in $C(m)$. Owing to the symmetry, each term that appears in the j series cancels itself with its counterpart in the i series. This kind of elimination is marked with $\langle 4 \rangle$ in Table 2, which signifies no more computation after $\langle 3 \rangle$.

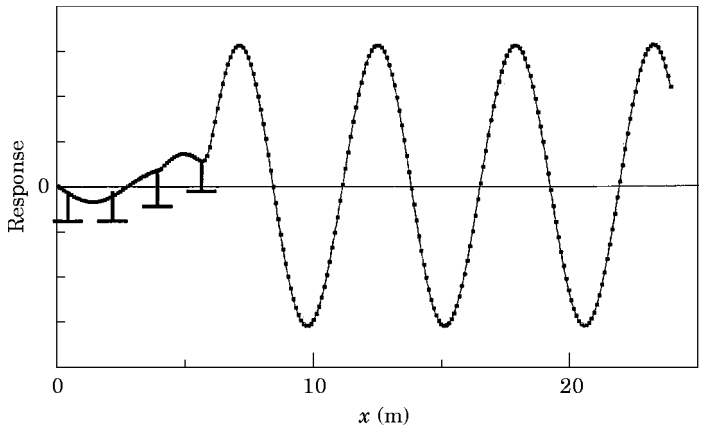

Figure 2. Mode shape at 35·00 Hz, close to a natural frequency of the damper $i = 4$.

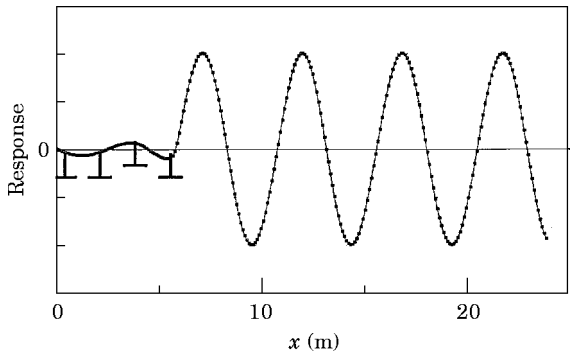

Figure 3. Mode shape at 38·79 Hz, close to a natural frequency of the damper $i = 1$.

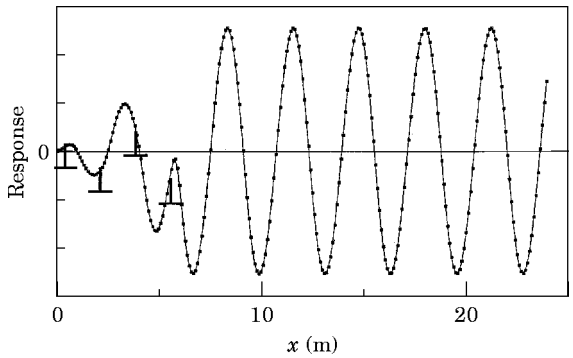

Figure 4. Mode shape at 60·00 Hz, close to a natural frequency of the damper $i = 2$.

4. NUMERICAL EXAMPLES AND DISCUSSION OF THE RESULTS

The conductor under consideration is an overhead ground wire with the following characteristics: span length $2L = 1050$ m, tension $S = 77250$ N, mass per unit length $M = 2{\cdot}23$ kg/m, diameter 0·025 m, bending stiffness $EJ = 1571$ Nm^2. At each of its two ends the conductor is laid on part of a circular (radius 1·52 m) attached to the suspension insulator hence it is approximately modelled as a beam with hinged ends.

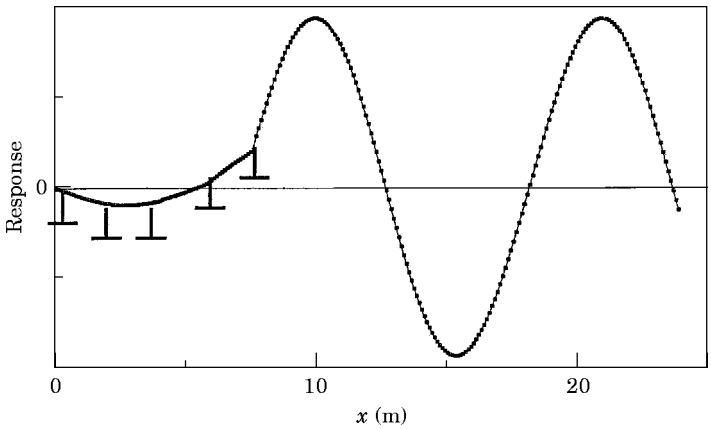

Figure 5. Mode shape at 20·49 Hz, close to a natural frequency of the damper $i = 1$.

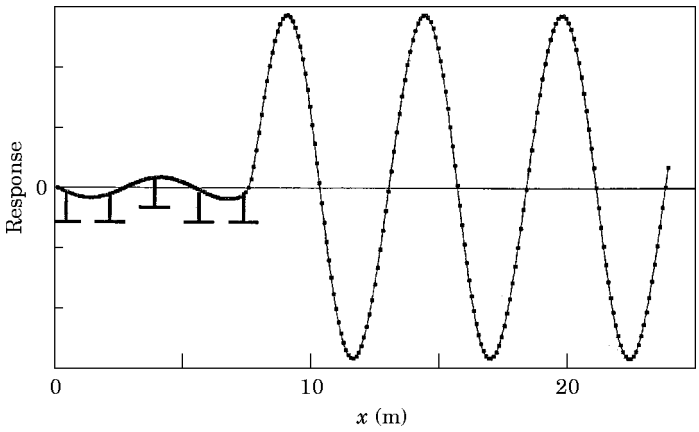

Figure 6. Mode shape at 35·00 Hz, close to a natural frequency of the damper $i = 5$.

Bending stiffness EJ was determined experimentally. The conductor-alone model was tested on a 45 m test span with the conductor held rigidly at terminals and tensioned with the exact value of S under consideration. The model was excited by an impact force which generated hundreds of peaks corresponding to natural frequencies of the span in the frequency spectrum. The spacing of each two adjacent peaks remained exactly uniform verifying the reliability of the data. The natural frequencies were employed to determine the value of EJ by using the tensioned clamped–clamped conductor-alone frequency equation which is quite simple. The value of EJ thus obtained lies well within the range between the so called EJ_{min} (based on the strands acting individually) and EJ_{max} (based on the assumption of no inter-strand slippage).

Four types of asymmetric Stockbridge dampers were used and the natural frequencies, i.e., the frequencies corresponding to the peaks of their force response, are listed in Table 3. The damper characteristics are listed in Table 4.

The numbers, types and locations of the dampers used in the computation are listed in Table 5.

Some of the mode shapes resulting from the computation are shown in Figures 2–8.

It is well recognized that a wind-induced transmission line vibrates in good agreement with one of the mode shapes. Consequently, once evaluated by aeolian vibration level

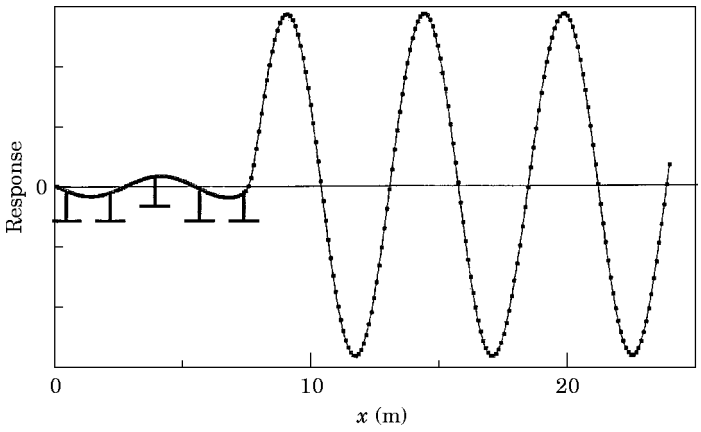

Figure 7. Mode shape at 35·08 Hz, close to a natural frequency in Figure 6.

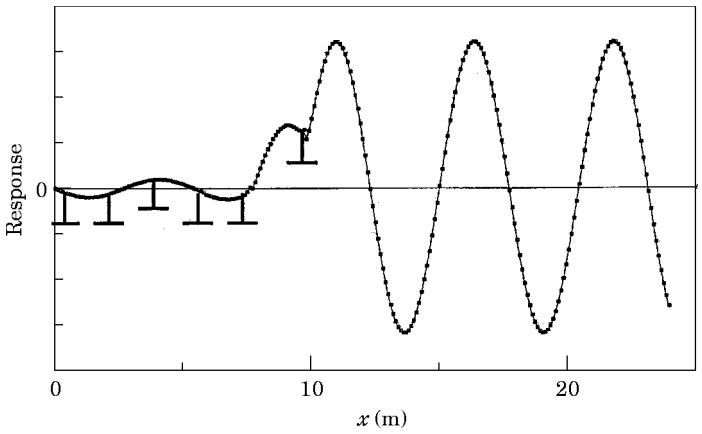

Figure 8. Mode shape at 35·00 Hz, close to a natural frequency of the damper $i = 5$.

computation using a certain method in the two groups mentioned in the Introduction, a mode shape represents the deformation distribution of the conductor vibrating with a frequency close to the natural frequency corresponding to the mode shape. The computation for natural frequency and mode shape thus provides an approach to estimating the overall strains of lines in operation or under design, including the dangerous strains. Since the mode shapes are given in the form of explicit and analytical functions, such estimation can be expressed simply by means of the second derivatives.

The computation indicates that the maximum curvature often takes place at the point of attachment of the last damper at a frequency in close vicinity to one of the natural frequencies of the damper as shown in the figures. This is why damage is often observed at such points. This kind of failure may suggest that the force response peaks of usual dampers are too sharp, so that damping in the damper as well as damping in the conductor is helpful. One can hardly detect any difference between curves in Figure 6 and Figure 7. They are mode shapes corresponding to two adjacent natural frequencies of the span. Searching for natural frequencies using frequency equations like equation (26) thus seems not necessary for long spans. On the other hand, mode shapes are quite sensitive to variation of tuning and location of the dampers (not shown in the figures). Careful design thus seems significant.

ACKNOWLEDGMENT

This work is part of a project supported by Hubei UHV Transformation and Transmission Bureau.

REFERENCES

1. C. Sahay 1991 *Shock and Vibration Digest* **23**(10), 8–13. Vibration of overhead transmission lines VI.
2. Y. T. Tsui 1982 *Electric Power Systems Research* **5**, 73–85. Recent advances in engineering science as applied to aeolian vibration: an alternative approach.
3. P. Hagedorn 1987 *Mathematical Modelling* **8**, 352–358. Wind-excited vibrations of transmission lines: a comparison of different mathematical models.
4. J. C. Roughan 1983 *Journal of Wind Engineering and Industrial Aerodynamics* **14**, 279–288. Estimation of conductor vibration amplitudes caused by aeolian vibration.

5. C. B. Rawlins 1983 *Institute of Electrical and Electronics Engineers*, *Transactions on Power Apparatus and Systems* **102**, 963–971. Wind tunnel measurements of the power imparted to a model of vibrating conductor.
6. R. Hartlen and I. Currie 1970 *Proceedings of the American Society of Civil Engineers* **96**, 577–591. Lift-oscillator model for vortex-induced vibration.
7. W. D. Iwan 1975 *Journal of Engineering for Industry* **97**, 1378–1382. The vortex induced oscillation of elastic structural elements.
8. R. A. Skop and O. M. Griffin 1975 *Journal of Sound and Vibration* **41**, 263–274. On a theory for the vortex-excited oscillations of flexible cylindrical structures.
9. A. Simpson 1972 *Journal of Sound and Vibration* **20**, 417–449. Determination of the natural frequencies of multi-conductor overhead transmission lines.
10. I. M. Babakov 1958 *Theory of Vibration* (in Russian). Moscow: State Publishing House.
11. T. S. Wu 1990 *Dissertation*, *Huazhong University of Science and Technology*. Aeolian vibration of long-span electrical transmission lines (in Chinese).
12. R. Claren and G. Diana 1969 *Institute of Electrical and Electronics Engineers*, *Transactions on Power Apparatus and Systems* **88**, 1741–1771. Mathematical analysis of transmission line vibration.

APPENDIX: FORCE RESPONSE OF A DAMPER

The asymmetric Stockbridge damper consists of two weights with different masses and different moments of inertia rigidly attached to the ends of a double cantilever of steel wire cable, which in turn is rigidly attached to the conductor cable by means of a clamp so as to form two cantilever systems with different arm lengths. Each cantilever system is a two-degree-of-freedom system and a damper is a four-degree-of-freedom system. The force response, i.e., the force amplitude generated by unit amplitude of its clamp motion, as derived in [11] is

$$q = \sum_{k=1}^{2} \frac{(4r_k\,\omega^2/\omega_k^2 - 4/3)\omega^2/\omega_k^2}{B_k\,/(M_k^2\,L_k^2\,\omega_k^2)}\,K_k$$

in which the subscript $k = 1, 2$ is referred to the two different sides of the damper, $r_k = \sqrt{I_k\,/M_k}/L_k$, I_k is the moment of inertia of one of the two weights, M_k is its mass, L_k is the arm length, ω is the circular frequency at which the damper clamp vibrates with the conductor cable, $\omega_k = \sqrt{K_k\,/M_k}$, $K_k = 3E_k\,J_k\,/L_k^3$, $E_k\,J_k$ is the bending stiffness of the steel wire cable, and

$$B_k = \{(4\omega_k^2 - \omega^2)\,[(4/3)\omega_k^2 - (r_k^2 + e_k^2\,/L_k^2)\omega^2] - [(e_k\,/L_k)\omega^2 - 2\omega_k^2]^2\}M_k^2\,L_k^2$$

in which e_k is the distance between the center of gravity of one of the two weights and its attachment point to the arm.